Figure 1. View of the Main Gulf Escarpment from the Gulf of California off the coast of Loreto. Credit: Rafael Sandaña via Wikimedia Commons.

Loreto, Mexico:
A Natural Laboratory for Study of the Interaction Between Faulting and Sedimentation

Lon D. Abbott*,[1] **and Terri L. Cook**[2]

GSA's 122nd annual Cordilleran Section Meeting in Loreto, Mexico, will unfold astride the Loreto normal fault, whose Pliocene motion raised the mountains west of town and formed the Loreto Basin in which the town nestles; Loreto owes its dramatic setting, where the mountains meet the sea (Fig. 1), to its namesake fault. The Loreto fault is the western rift-bounding fault along which Baja separated from mainland Mexico during opening of the Gulf of California (Fig. 2). Loreto is an especially fitting venue for tectonics- and sedimentation-focused technical sessions, short courses, and field trips because the Loreto Basin and its surroundings constitute a world-class natural laboratory in which to study interactions between faulting and sedimentation. Details of the basin's sedimentary architecture record variations in past fault slip rates; Pliocene strata on nearby Isla del Carmen provide mute testimony to the tectonic beheading of its drainage network; and seismic detective work on an 1810 earthquake and tsunami revealed the timing of a submarine landslide that would otherwise have gone undetected.

LORETO'S TECTONIC TRANSFORMATION: FROM SUBDUCTION TO RIFT ZONE

The Baja Peninsula's bedrock spine consists of Cretaceous granites belonging to the Peninsular Ranges Batholith, which formed during Farallon plate subduction beneath North America. That long-lived subduction was disrupted when the Farallon-Pacific plate spreading center reached the trench at ~28 Ma near the latitude of the international border (Fig. 2). That first contact between the Pacific and North American plates grew in length through time as the Mendocino triple junction migrated north and the Rivera triple junction migrated south, extending the San Andreas transform fault and extinguishing the volcanic arc as they traveled. The Rivera triple junction reached the latitude of central Baja by 16 Ma and the peninsula's southern tip by 10 Ma, transforming Baja from a subduction zone to a place of right-lateral strike-slip motion combined with extension (transtension; Fig. 2), opening the proto-Gulf of California as it went (Lonsdale, 1991; Sedlock, 2003).

---

*lon.abbott@colorado.edu
[1] Department of Geological Sciences, University of Colorado, Boulder, Colorado 80309, USA
[2] Down to Earth Science, Boulder, Colorado 80305, USA

CITATION: Abbott, L.D., and Cook, T.L., 2026, Loreto, Mexico: A natural laboratory for study of the interaction between faulting and sedimentation: GSA Today, v. 36, p. 28–31, https://doi.org/10.1130/GSATG123GH.1

The Mexican volcanic arc associated with Farallon subduction simultaneously migrated westward from a ~25 Ma locus in mainland Mexico's Sierra Madre Occidental to the modern Loreto coast by 12 Ma. The 30–12 Ma volcanic and volcaniclastic rocks of the Comondú Group, which unconformably overlie Cretaceous granite in the Loreto area, record that short-lived Oligo-Miocene arc's westward wanderings (Umhoefer et al., 2001).

Following passage of the Rivera triple junction, movement began ~8–6 Ma on the 35-km-long oblique-slip Loreto fault to accommodate the new transtensional tectonic setting (Mark et al., 2014). Uplift of the fault's footwall raised the Main Gulf Escarpment, the imposing mountain range west of Loreto; hangingwall subsidence created the Loreto Basin (Fig. 3; Dorsey and Umhoefer, 2000) east of the fault. Continental rifting evolved to seafloor spreading in the Gulf of California sometime between ~6–2.5 Ma, but normal faulting continues today from Loreto southward (Fig. 2). This simultaneous "rifting-while-drifting" defies the conventional wisdom that the transition from continental rifting to seafloor spreading is a discrete event (Umhoefer et al., 2020).

FROM STACKED GILBERT DELTAS TO SEISMIC SWARMS

Slip on the Loreto fault ended by ~2 Ma as extension shifted eastward to faults along the modern Gulf coastline and farther offshore. That shift was fortuitous, as it placed the Loreto Basin in the new fault's rising footwall, where it was uplifted and dissected, allowing geologists to scrutinize its Pliocene basin fill. It consists of two subbasins—the central and southeast—that share a common four-sequence stratigraphy, but the southeast subbasin's sedimentary column is thinner. Its sequence architecture also differs markedly from its central subbasin sibling, revealing that the northern and southern portions of the Loreto fault slipped at different rates (Dorsey et al., 1995; Dorsey and Umhoefer, 2000).

Four tuff beds in the central subbasin have been $^{40}Ar/^{39}Ar$ dated, enabling geologists to reconstruct the area's sedimentation rates. Tuff #1, near the base of Sequence 2, erupted 2.61 Ma, and tuff #2, 64 m higher in the section, is 2.46 Ma, indicating an accumulation rate of ~0.4 mm/yr. Tuff #3 is 765 m higher, near the base of Sequence 4, but is a mere 100 k.y. younger at 2.36 Ma, requiring a much faster sediment accumulation rate of 8 ± 5 mm/yr. The range in rates is due to the dates' analytical uncertainties. Finally, tuff #4, near the top of Sequence 4, 160 m above, is 1.97 Ma (Umhoefer et al., 1994), documenting that the sedimentation rate had returned to ~0.4 mm/yr during Sequence 4 deposition.

Combined analysis of basin architecture and accumulation rates has enabled geologists to reconstruct a detailed slip history for the Loreto fault. Sequence 1 consists of nonmarine conglomerate whose provenance and paleocurrents indicate two source directions—from the Main Gulf Escarpment in the west and from the coastal Sierra Microondas massif, 10 km north of Loreto, in the east. The fill is exclusively nonmarine, showing that sedimentation easily kept pace with both basin subsidence and eustatic sea-level fluctuations, which dictates that the fault slip rate was modest (Fig. 3A). But subsidence had to keep pace with sedimentation to create accommodation space, so the fault slip rate 2.6–2.46 Ma (Umhoefer et al., 1994) was ~0.4 mm/yr. Provenance analysis suggests a similar slip rate was maintained from fault inception to the start of Sequence 2 (Mortimer and Carrapa, 2007).

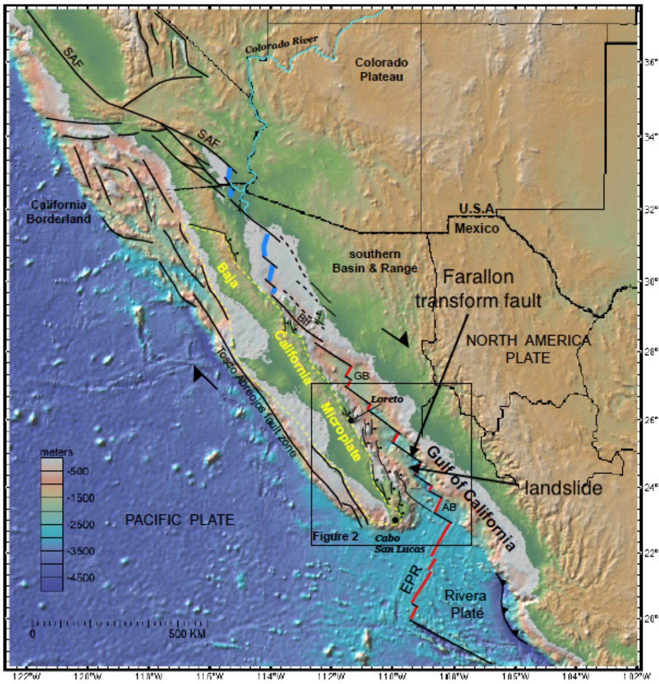

Figure 2. Tectonic map of the Gulf of California plate boundary, with Loreto, the Farallon transform, and tsunami-generating landslide location marked. Black lines are transform faults, black lines with the ball-and-stick pattern are normal faults with the ball-and-stick on the hangingwall, red lines are spreading centers, and blue lines are nascent or buried spreading centers. SAF = San Andreas fault, GB = Guaymas basin, AB = Alarcón basin, EPR = East Pacific Rise, Btf = Ballenes transform fault. Credit: Umhoefer et al. (2020).

The Sequence 1–2 boundary is a marine shell bed that records abrupt drowning of the basin. The age of tuff #1, just above the sequence boundary, implies that a 2.62 Ma eustatic sea-level rise (Raymo et al., 1992) triggered the flooding event (Dorsey and Umhoefer, 2000). Soon thereafter the central subbasin sedimentation rate increased abruptly to 8 ± 5 mm/yr; a commensurate increase in basin subsidence rate was necessary to produce the required accommodation space (Fig. 3B). The central subbasin's Sequence 2 consists of 14 stacked Gilbert deltas containing both nonmarine and marine conglomerate and turbidites with steep foresets up to 35 m tall (Dorsey and Umhoefer, 2000; Mortimer et al., 2005). Each delta prograded 1–2 km into the basin, then was drowned by a rapid transgression marked by a marine shell bed. Each cycle of delta construction and drowning unfolded in just a few thousand years, much too fast to be explained by 41 k.y. glacio-eustatic sea-level changes driven by Milankovitch cycles (Raymo et al., 1992). Instead, researchers conclude the stacked Gilbert deltas record brief periods of rapid fault slip, with the slip rate fluctuating from <2 mm/yr to 8 mm/yr across the duration of a cycle (Mortimer et al., 2005). Basins produced by strike-slip faulting have long been known to experience brief periods of rapid subsidence; the Loreto Basin's stratigraphic relationships allowed such behavior in an ancient basin to be quantified for the first time (Dorsey et al., 1995, 1997). Numerical fault models predict the occurrence of episodic earthquake swarms across families of normal faults, like the family here in southern Baja (Fig. 2). Seismic swarms are triggered in the model by complex stress interactions between faults (Cowie, 1998); the activity of past swarms provides a plausible explanation for the central Loreto Basin's cycles of fast and slow subsidence (Mortimer et al., 2005).

In contrast to the central subbasin, Sequence 2 possesses only four sediment packages separated by flooding surfaces in the southeastern subbasin. These four local transgressions nicely match the four eustatic transgressions recorded in the marine isotopic record during the interval of Sequence 2 deposition. The southern Loreto Fault was slipping then at ~1.5 mm/yr, a rate slow enough that fault slip was unlikely to overwhelm the sedimentary signal recorded by glacio-eustatic sea-level fluctuations (Dorsey and Umhoefer, 2000).

Paleocurrent data reveal that the eastern sediment source active during Sequence 1 (Fig. 3A) shut off during Sequence 2 (Fig. 3B) but was reactivated during Sequence 3 deposition (Fig. 3C). Shutdown of the source was likely due to rapid subsidence during Sequence 2. Researchers hypothesize its rejuvenation was likely caused by initiation of a new fault east of the Loreto Basin 2.37 Ma, which placed the basin on that fault's rising footwall, thus re-exposing the Sierra Microondas source. Sequence 4 records deepening of the central subbasin to 100–150 m water depth, which likely records a final spasm of rapid slip 2.36–2.0 Ma, before Loreto Fault activity ceased (Dorsey and Umhoefer, 2000).

ISLA DEL CARMEN: A TECTONIC DECAPITATION

Isla del Carmen, the fourth-largest island in the Gulf of California, lies 20 km east of Loreto. Marine terraces as old as 400 ka (marine isotope stage 11) and up to 68 m elevation are etched on the island's limestone flanks, recording recent tectonic uplift (Johnson et al., 2016). Paleomagnetic data indicate the island has also rotated 30–40° clockwise, which accounts for its unusual NE-SW orientation compared to the typical NW-SE trend of other Gulf islands. Its northwest and southeast coasts are bounded by normal faults that GPS data show are currently pulling the island away from Baja toward the southeast at 3.2 ± 1.8 mm/yr (Umhoefer et al., 2020). The island's stratigraphy helps constrain when it first separated from the peninsula.

The Tiombó conglomerate fills a broad channel across the island that's interpreted to be a middle Pliocene (~3.6 Ma) fan delta with an estimated volume >200 million m^3. That is much too large to be sourced from the island's diminutive drainage basins, which means the island remained connected to the Baja peninsula throughout the middle Pliocene. Based on the delta's size and orientation, researchers suggest that modern arroyos stretching from Loreto to just south of the town of Nopoló once converged in what is today the Carmen Passage and flowed east to feed the island's delta. They estimate the paleodrainage basin area at 525 km^2, which is 400 km^2 larger than the modern Loreto delta (Johnson et al., 2016).

The presence of the Tiombó fan delta implies that the current normal fault separating the island from Loreto, whose hangingwall subsidence drowned the Carmen Passage, is younger than 3.6 Ma. That fault's initiation in later Pliocene or Pleistocene time then decapitated the delta (Johnson et al., 2016).

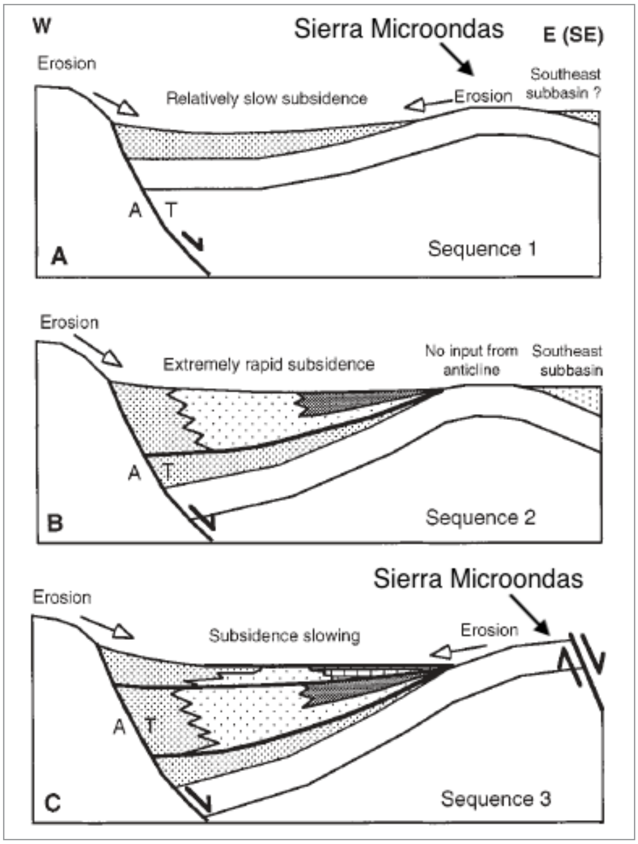

Figure 3. Schematic cross section depicting the evolution of the central subbasin of the Loreto basin. (A) Slow slip on the Loreto normal fault results in slow basin subsidence during deposition of Sequence 1. Paleocurrents reveal two sediment sources, from the Main Gulf Escarpment west of the Loreto fault and from the Sierra Microondas to the east. (B) Accelerated slip on the Loreto fault produces rapid basin subsidence during Sequence 2 deposition. The eastern sediment source has shut off. (C) Slip on the Loreto fault has slowed once again during deposition of Sequence 3. The Sierra Micoondas sediment source has been rejuvenated by uplift on the footwall of a new normal fault to the east. The dense stippled pattern denotes terrestrial conglomerate deposition, the lighter stipple is marine conglomerate of Gilbert delta foresets, and the gray shading marks distal marine turbidites. Credit: Dorsey and Umhoefer (2000).

In addition to recording a tectonic decapitation, the Isla del Carmen stratigraphy also records clues to Baja's paleoclimate. Seemingly paradoxically, the Tiombó fan delta grew adjacent to rhodolith-bearing limestones, which form only in clear, low-turbidity waters (Johnson et al., 2016). Pliocene Loreto Basin sediments likewise contain a mixture of mollusk-rich bioclastic limestone and volcaniclastics, a combination that requires juxtaposition of abundant clastic sedimentation with a clear water carbonate factory. Upwelling of cool, nutrient-rich water has been invoked to explain the abundant Pliocene mollusks (Dorsey and Kidwell, 1999). Aridity punctuated by more frequent hurricanes than occur today, a feature of the sustained El Niño-like climate that models predict characterized the Pliocene Warm Period, could plausibly produce the voluminous clastic sediment needed to feed large Pliocene fan deltas while maintaining a clear water carbonate factory most of the time (Johnson et al., 2016).

THE TSUNAMI THAT SHOULDN'T HAVE HAPPENED

A major earthquake (estimated at Mw = 7.4) shook Loreto on 27 August 1810. The earthquake, combined with a tsunami that arrived one hour later and surged up to 5 km inland, caused considerable damage along 200 km of the eastern Baja coastline. Strong earthquakes have been common in the Loreto area since European arrival (Suter, 2018), but tsunamis are rare (Ramírez-Herrera et al., 2019) due to the predominantly strike-slip nature of Gulf seismicity (Umhoefer et al., 2020).

Analysis of Loreto's historical seismicity indicates a puzzle: the 1810 earthquake nucleated on the right-lateral Farallon transform fault (Fig. 2; Suter, 2018), but the tsunami's estimated 25-m height far exceeded the <1.5-m height that models predict for a magnitude 7.4 strike-slip earthquake. Equally mysterious is the 1 h delay between the quake and the tsunami's arrival; a wave produced at the Farallon fault should reach Loreto in just 24 min. What could account for these discrepancies? Ramírez-Herrera et al. (2019) decided to do some seismic sleuthing. They postulated that a submarine landslide triggered by the earthquake was responsible for the tsunami, rather than the earthquake itself. Their scrutiny of Gulf of California bathymetry revealed 22 candidate submarine landslide scars, each of which they modeled as a potential tsunami source. The best-fit candidate, which matches the amplitude and timing of the 1810 tsunami, is a 21 km × 12 km slump 70 km northeast of the coastal town of Tembabichi, 80 km south of Loreto (Ramírez-Herrera et al., 2019).

Loreto's combination of tectonic dynamism and arid-region sedimentary processes has produced an exquisite natural laboratory that enables geologists to probe interactions between faulting and sedimentation in fine detail. Past work has constrained the timing of one fault's initiation, identified a past earthquake as the trigger for a specific mass-wasting deposit, and quantified ancient fault slip rates in unprecedented detail. We look forward to reading about the future groundbreaking research that will undoubtedly be inspired by the gathering of geoscientists in this place of noteworthy geoheritage for GSA's 122nd annual Cordilleran Section Meeting.

REFERENCES CITED

Cowie, P.A., 1998, A healing-reloading feedback control on the growth rate of seismogenic faults: Journal of Structural Geology, v. 20, p. 1075–1087, https://doi.org/10.1016/S0191-8141(98)00034-0.

Dorsey, R.J., and Umhoefer, P.J., 2000, Tectonic and eustatic controls on sequence stratigraphy of the Pliocene Loreto basin, Mexico: GSA Bulletin, v. 112, p. 177–199, https://doi.org/10.1130/0016-7606(2000)112<177:TAECOS>2.0.CO;2.

Dorsey, R.J., and Kidwell, S.M., 1999, Mixed carbonate-siliciclastic sedimentation on a tectonically active margin: Example from the Pliocene of Baja California Sur, Mexico: Geology, v. 27, p. 935–938, https://doi.org/10.1130/0091-7613(1999)027<0935:MCSSOA>2.3.CO;2.

Dorsey, R.J., Umhoefer, P.J., and Renne, P.R., 1995, Rapid subsidence and stacked Gilbert-type fan deltas, Pliocene Loreto Basin, Baja California Sur, Mexico: Sedimentary Geology, v. 98, p. 181–204, https://doi.org/10.1016/0037-0738(95)00032-4.

Dorsey, R.J., Umhoefer, P.J., and Falk, P., 1997, Earthquake clustering and stacked Gilbert-type fan deltas in the Pliocene Loreto Basin, Baja California Sur, Mexico: Geology, v. 25, p. 679–682, https://doi.org/10.1130/0091-7613(1997)025<0679:ECIFPG>2.3.CO;2.

Johnson, M.E., Ledesma-Vázquez, J., and Backus, D.H., 2016, Tectonic decapitation of a Pliocene mega-delta on Isla Del Carmen in the Gulf of California (Mexico): And a river ran through it: The Journal of Geology, v. 124, p. 55–74, https://doi.org/10.1086/684206.

Lonsdale, P., 1991, Structural patterns of the Pacific floor offshore of Peninsular California, *in* Dauphin, J.P., and Simoneit, B.T., eds., Gulf and Peninsula Province of the Californias: American Association of Petroleum Geologists Memoir 47, p. 87–125, https://doi.org/10.1306/M47542C7.

Mark, C., Gupta, S., Carter, A., Mark, D.F., Gautheron, C., and Martin, A., 2014, Rift flank uplift at the Gulf of California: No requirement for asthenospheric upwelling: Geology, v. 42, p. 259–262, https://doi.org/10.1130/G35073.1.

Mortimer, E., and Carrapa, B., 2007, Footwall drainage evolution and scarp retreat in response to increasing fault displacement: Loreto fault, Baja California Sur, Mexico: Geology, v. 35, p. 651–654, https://doi.org/10.1130/G23690A.1.

Mortimer, E., Gupta, S., and Cowie, P.A., 2005, Clinoform nucleation and growth in coarse grained deltas, Loreto basin, Baja California Sur, Mexico: A response to episodic accelerations in fault displacement: Basin Research, v. 17, p. 337–359, https://doi.org/10.1111/j.1365-2117.2005.00273.x.

Ramírez-Herrera, M.T., Corona, N., and Castillo-Aja, R., 2019, Revealing the source of the 27 August 1810 Loreto, Baja California, tsunami from historical evidence and numerical modelling: Pure and Applied Geophysics, v. 176, p. 2951–2967, https://doi.org/10.1007/s00024-019-02161-z.

Raymo, M.E., Hodell, D., and Jansen, E., 1992, Response of deep ocean circulation to initiation of Northern Hemisphere glaciation (3–2 Ma): Paleoceanography, v. 7, p. 645–672, https://doi.org/10.1029/92PA01609.

Sedlock, R.L., 2003, Geology and tectonics of the Baja California peninsula and adjacent areas, *in* Johnson, S.E., Paterson, S.R., Fletcher, J.M., Girty, G.H., Kimbrough, D.L., and Martín-Barajas, A., eds., Tectonic Evolution of Northwestern México and the Southwestern USA: Geological Society of America Special Paper 374, p. 1–42, https://doi.org/10.1130/0-8137-2374-4.1.

Suter, M., 2018, The historical seismicity of the Loreto Region, Baja California Peninsula, Mexico (1684–1878): Seismological Research Letters, https://doi.org/10.1785/0220170204.

Umhoefer, P.J., Dorsey, R.J., and Renne, P., 1994, Tectonics of the Pliocene Loreto basin, Baja California Sur, Mexico, and the evolution of the Gulf of California: Geology, v. 22, p. 649–652, https://doi.org/10.1130/0091-7613(1994)022<0649:TOTPLB>2.3.CO;2.

Umhoefer, P.J., Dorsey, R.J., Willsey, S., Mayer, L., and Renne, P., 2001, Stratigraphy and geochronology of the Comondú Group near Loreto, Baja California Sur, Mexico: Sedimentary Geology, v. 144, p. 125–147, https://doi.org/10.1016/S0037-0738(01)00138-5.

Umhoefer, P.J., Plattner, C., and Malservisi, R., 2020, Quantifying rates of "rifting while drifting" in the southern Gulf of California: The role of the southern Baja California microplate and its eastern boundary zone: Lithosphere, v. 12, p. 122–132, https://doi.org/10.1130/L1132.1.